Catalytic and EPR Studies of the βE204Q Mutant of the Chloroplast F_1-ATPase from *Chlamydomonas reinhardtii*†

Chia-Yuan Hu,‡,§ Andrew L. P. Houseman,§,|| Lola Morgan,§,|| Andrew N. Webber,§,|| and Wayne D. Frasch*,§,||

The Department of Chemistry and Biochemistry, The Center for the Study of Early Events in Photosynthesis, and The Department of Botany, Arizona State University, Box 871601, Tempe, Arizona 85287-1601

Received May 8, 1996⊗

ABSTRACT: The mutation E204Q in the β subunit of the chloroplast F_1-ATPase was made by biolistic transformation of *Chlamydomonas reinhardtii*. The yield of chloroplast F_1-ATPase (CF_1) purified from thylakoids was unaltered, suggesting that the mutation did not affect protein assembly. However, photoautotrophic growth of *Chlamydomonas* strains containing βE204Q was virtually abolished, and the effect of the mutation on the light-driven ATPsynthase activity catalyzed by purified thylakoids was comparable to the change in the photoautotrophic growth rate. The loss of ATPsynthase activity in the mutant was not the result of uncoupling. Addition of wild-type CF_1 to mutant thylakoids depleted of CF_1 reconstituted ATPsynthase activity indicating that the mutation did not affect assembly of F_0. Furthermore, the mutant CF_1F_0 was capable of catalyzing ATPase-dependent proton pumping as measured by fluorescence quenching of 9-amino acridine. Although the mutation significantly affected the apparent k_{cat}/K_M of the Mg^{2+}-ATPase activity of the purified CF_1-ATPase, no significant effect on the apparent k_{cat} was observed with the mutant compared to wild-type. No significant changes in the ability of Mg^{2+} or Mn^{2+} to serve either as a cofactor or as an inhibitor of ATPase activity were observed in the mutants relative to the wild-type CF_1-ATPase. EPR spectra were also taken of VO^{2+} bound at catalytic site 3 in its latent form. In a large fraction of the latent enzyme, a carboxyl group has displaced the nucleotide−phosphate coordination to the metal which results in the free-metal inhibited form (M3). No significant effects on the $g_{||}$ and $A_{||}$ ^{51}V hyperfine parameters were observed between wild-type and mutant. However, the mutation increased the abundance of the M3 form relative to the M3−N3 form (metal−nucleotide-coordinated form). On the basis of these results, βE204 is not the carboxyl group that displaces the nucleotide phosphate as a ligand to form the free-metal inhibited enzyme form which predominates in site 3 in the latent state. Instead, the data are consistent with a role in which βE204 is essential to protonate an inorganic phosphate−oxygen to make that oxygen a good leaving group to facilitate ATP synthesis and, via this role in H-bonding, increases the abundance of the functional metal−nucleotide complex bound to the catalytic site.

The F_1F_0-ATPsynthase[1] couples proton translocation across membranes with the synthesis or hydrolysis of ATP. In the chloroplast, the light-driven generation of a proton gradient is used by the enzyme as an energy source for ATP synthesis (Frasch, 1994). Dissipation of the proton gradient through the membrane-embedded F_0 proton channel couples the energy in the gradient to the synthesis of ATP. The F_1 is an extrinsic membrane protein complex which has three catalytic sites primarily associated with the β subunits and is still capable of ATPase activity after purification from the membrane. The subunits of the F_1-ATPase from chloroplast, mitochondrial, and bacterial origin share a high degree of amino acid sequence homology, the β subunit having the highest homology (Walker et al., 1985).

Each active site catalyzes the net reaction

$$ADP + P_i + 2H^+ \Leftrightarrow ATP + H_2O \qquad (1)$$

in a reversible manner such that the equilibrium constant of the bound reactants and products rapidly approaches unity without the input of energy (Boyer et al., 1993). The reaction is facilitated by a metal cofactor like Mg^{2+} that coordinates the phosphate oxygens with a specific stereochemistry (Frasch & Selman, 1982). The F_1 catalyzes a direct, in-line transfer of the phosphoric residue between the bound ADP and water (Webb et al., 1980; Senter, 1983). Thus, to catalyze the synthesis of ATP, one or two amino acid residues are required to protonate an oxygen of the inorganic phosphate to make that oxygen a good leaving group and allow a nucleophilic attack by the β-phosphate oxygen of ADP. Since the reaction occurs with inversion of configuration, the residue(s) must be positioned on a face of the inorganic phosphate that is distal from the ADP. Several independent lines of evidence concur that the protons from

† This research was supported by grants from the United States Public Health Service (GM50202) and the H. Frasch Foundation (0188HF) to W.D.F. and the U.S. Department of Agriculture NRIC Grants 92-01249 to W.D.F. and 93-37306-6473 to A.N.W. L.M. is a Howard Hughes Medical Institute Research Fellow supported by a grant from the HHMI through the Biological Sciences Education Program. This is publication 301 of the Center for the Study of Early Events in Photosynthesis.

* Author to whom correspondence should be addressed.

‡ The Department of Chemistry and Biochemistry.

§ The Center for the Study of Early Events in Photosynthesis.

|| The Department of Botany.

⊗ Abstract published in *Advance ACS Abstracts,* August 15, 1996.

[1] Abbreviations: DCCD, dicyclohexylcarbodiimide; F_1, the solubilized ATPase portion of the F_1F_0-ATPsynthase, CF_1, F_1 from chloroplasts; EF_1, F_1 from *E. coli*; MF_1, F_1 from mitochondria; TF_1, F_1 from the thermophilic bacterium *PS3*; AMP-PNP, 5′-adenylyl imidodiphosphate; PMS, phenazine methylsulfate; PSI, photosystem I; PCR, polymerase chain reaction; CD, circular dichroism.

S0006-2960(96)01105-1 CCC: $12.00

the transmembrane proton gradient are not consumed in the condensation reaction during ATP synthesis shown in eq 1, but rather drive a conformational change of the protein that facilitates the release of ATP.

In the crystal structure of the F_1-ATPase from bovine heart mitochondria (MF_1), the catalytic site that contains bound AMP-PNP shows density for a bound water 4.4 Å from the γ-phosphate of the nucleotide (Abrahams et al., 1994). This water is hydrogen-bonded to βE188 such that this residue is in a position that could activate the water molecule to promote a nucleophilic attack on the terminal phosphate. However, this residue is also close enough to the bound metal at this site to serve as a metal ligand in this or another catalytic site. Houseman et al. (1995) suggested that this may be the residue that contributes a carboxylate to the coordination sphere of metal at the catalytic site in the "free-metal-inhibited" form.

Dicyclohexylcarbodiimide (DCCD) modifies specific carboxyl-residues of the β subunit from mitochondria, bacteria, and the chloroplast F_1 in a manner that inactivates the enzyme (Pougeois et al., 1979; Shoshan et al., 1980; Yoshida et al., 1981). In TF_1 from the thermophilic bacterium *PS3*, DCCD covalently modifies the carboxyl residue at the position equivalent to βE188 in MF_1 (Yoshida et al., 1980). Modification of nearby residues in the F_1-ATPases from EF_1, the enzyme from *Escherichia coli* (Esch et al., 1981), and CF_1, the spinach chloroplast enzyme (Sakurai et al., 1989), by a single equivalent of DCCD is sufificient to inactivate CF_1 completely and to eliminate a high-affinity nucleotide-binding site (Shoshan et al., 1980). The presence of Mg^{2+} interfered with inactivation of CF_1 by DCCD, suggesting that the modified residue was involved in metal binding at the metal−nucleotide binding site (Vallejos, 1981). A metal-binding role for these carboxyl groups was also suggested by the observation that while the binding of a single ADP to TF_1 accelerated DCCD-modification, the presence of Mg^{2+} abolished the effect of ADP (Yoshida & Allison, 1986). However, other work has shown that, although the nucleotide is unable to bind after DCCD modification, the binding of metal is unaffected (Dagget et al., 1985).

Site-directed mutations that involve the substitution of a glutamine for the glutamate at position 181 (equivalent to βE188 in MF_1) in the β subunit of EF_1 resulted in about a 1000-fold decrease in Mg^{2+}-ATP binding and catalytic activity (Senior & Al-Shawi, 1992; Amano et al., 1994; Park et al., 1994). Under conditions in which only one catalytic site is filled with ATP (unisite conditions), comparison of the rate constants of the individuals steps in the ATPase reaction for the wild-type and βE181Q mutant enzymes showed that the mutation affected all the ground states and transition states significantly, but affected the catalytic interconversion step in particular (Senior et al., 1992; Park et al., 1994). On the basis of similar results from the same mutant of EF_1, Park et al. (1994) speculated that βE181 was a candidate for activation of a water molecule for nucleophilic attack on ATP. However, both groups concluded that the data supported βE181 as a Mg^{2+} ligand (Park et al., 1994; Al-Shawi et al., 1990).

Individual high-affinity sites in CF_1 can be selectively depleted and filled with metal and nucleotide (Bruist & Hammes, 1981). We have used this property of CF_1 to investigate the metal-binding sites of the F_1-ATPase. Using the paramagnetic Mg^{2+} analog vanadyl $(V^{IV}{=}O)^{2+}$, Houseman et al. (1994a,b) recently examined the metal-binding sites of CF_1 with EPR spectroscopy. In the activated form of the enzyme, the ligands to the VO^{2+} at catalytic site 3 do not include a carboxyl group when the metal is bound as the metal−nucleotide complex, M3−N3. In the latent form, the catalytic site has two forms of bound metal. Latent site 3 can bind both nucleotide and Mg^{2+} in the M3−N3 form in which nucleotide is coordinated to the metal, but a comparable amount of bound Mg^{2+} is in the M3 form, the "free-metal-inhibited" form, in which the phosphates of the nucleotide do not coordinate the metal. Instead, the composite of metal ligands is the same as when metal is bound to the site in the absence of nucleotide. A carboxyl group probably does serve as one of the equatorial ligands to VO^{2+} bound to the catalytic site under these conditions. Thus, free-metal inhibition and reversion to the latent state both appear to be related to the metal coordinating the carboxyl group in lieu of the phosphates of the nucleotide. Inhibition by free-metal binding would be particularly effective if the coordinating carboxyl group were also the one responsible for activating the phosphate oxygen to make it a good leaving group during ATP synthesis.

Few mutatations have been made or characterized in the chloroplast F_1-ATPase, even though it has been possible to create site-directed mutations in the chloroplast genome in *Chlamydomonas* (Boynton et al., 1988). We now report the characterization of the site-directed mutation that replaces glutamate with glutamine at position 204 in the β subunit of the chloroplast F_1 complex of *Chlamydomonas reinhardtii* (equivalent to residue 181 in EF_1) biochemically and by EPR spectroscopy of VO^{2+} bound at a single catalytic site. Our results strongly suggest that this residue is not a metal ligand, but it does increase the fraction of bound metal and nucleotide that exist as a complex in catalytic site 3 of the latent enzyme.

EXPERIMENTAL PROCEDURES

Strains and Culture Media. *C. reinhardtii* strains were obtained from the *Chlamydomonas* Culture Collection at Duke University. CC-125 is a wild-type mt^+ strain (Harris, 1989). CC-373 (*ac-u-c*-221) is a non-photosynthetic strain that carries a 2.5 kb deletion in the chloroplast *atpB* gene (Boynton et al., 1988). The CC-373 (*au-u-c*-221) strain has been transformed with the wild-type chloroplast *atpB* gene and is referred to as WT-373. The cells were maintained on HS (Sueoka, 1960) media supplemented with acetate (HSA).

Plasmids, in Vitro Mutagenesis, and Chloroplast Transformation. A 5.3 kilobase pair (kb) *Eco*RI−*Bam* fragment designated *Bam*-10.3 was isolated from the chloroplast DNA *Bam* restriction fragment *Bam*-10 containing the *atpB* gene and was subcloned into pUC19. A 2.9 kb *Eco*RI−*Kpn*I from *Bam*-10.3 was then isolated and cloned into M13mp19. The single-strand DNA from this bacteriophage plasmid was used as a template for oligonucleotide-mediated site-directed mutagenesis. The mutagenic oligonucleotide was 5′ GGT GTT GGT G(C)AA CGT ACA CGT GAA GGT AAC GAC CTT TAC ACA GAA ATG AAA GAA TCT GGT 3′. The primer was designed to change glutamate β204 to glutamine. The mutation introduced into codon 610 (Woessner et al., 1986) to obtain the β204Q mutant was performed with the Amersham kit RPN-1523 following manufacturer's protocols.

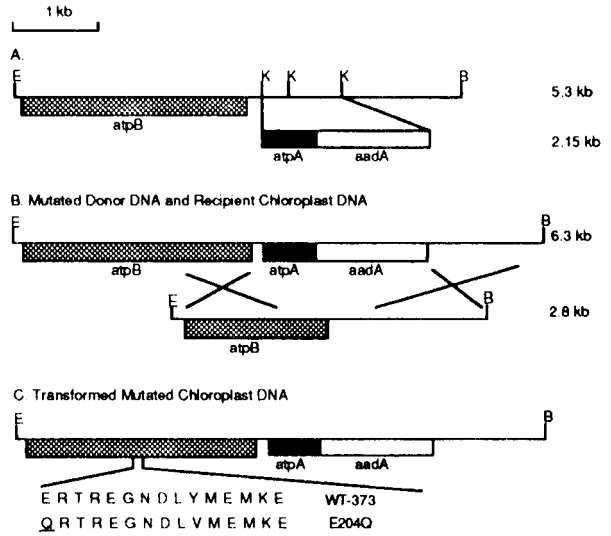

FIGURE 1: Restriction enzyme map of *Eco*RI−*Kpn*I fragment from *C. reinhardtii atpB* gene and the locations of inserted *atpA-aadA-rbcL* cassette and mutated residues. (A) The 5.3 kb *Eco*RI−*Bam*HI from chloroplast DNA fragment *Bam*-10 containing *atpB* as well as restriction sites for the following: E, *Eco*RI; K, *Kpn*I; and B, *Bam*HI. (B) Placement of the 2.15 kb *atp*A-*aad*A cassette conferring the specintomycin resistance into 1.15 kb *Kpn*I fragment deletion region. The 6.3 kb spectinomycin resistance *Eco*RI−*Bam*HI fragment containing the mutated *atpB* gene was cloned into pUC19 to make the donor plasmid pβE204Q. CC-373, which lacks 2.5 kb of *Bam*-10 including the 3′ end of *atpB*, was used as recipient of the donor plasmid DNA. (C) Amino acid sequence of the mutated carboxyl residue in β subunit of *C. reinhardtii* chloroplast CF_1.

After site-directed mutagenesis, the *Eco*RI−*Kpn*I fragment containing the desired mutation was subcloned into *Bam*-10.3. A 2.15 kb DNA fragment with the *atpA-aadA-rbcL* cassette was used to replace the 1.15 kb *Kpn*I fragment in the mutated *Bam*-10.3 by blunt-end ligation (Woessner et al., 1986). The *aadA* gene conferred spectinomycin resistance (Goldschmidt-Clermont, 1991), *atpA* functioned as a promoter of the *aadA* gene, and the 3′ end of the *rbcL* gene was used to stabilize this cassette. The final mutated plasmid construct was designated pβE204Q. Replacement of the 1.15 kb *Kpn*I fragment of wild-type *Bam*-10.3 with the 2.15 kb *atpA-aadA-rbcL* cassette resulted in a plasmid construct pWT-373, which was used to obtain the WT-373 strain. The WT-373 strain was used as a control for photosynthetic measurements.

Biolistic transformation of *C. reinhardtii* was performed following procedures previously described (Boynton et al., 1988; Webber et al., 1993) for chloroplast transformation. The CC-373 strain of *C. reinhardtii* contains a 2.5 kb deletion of *Bam*-10 including the 3′ end of the *atpB* gene. This was used as a recipient in the transformation experiment (Figure 1). CC-373 cells were grown to approximately 3×10^6 in the HSA medium as described (Harris, 1989). The cells were then concentrated and resuspended in HSA medium to a concentration of 5×10^7 cells per mL. Cells in 0.5 mL volume were spread evenly on plates (CC plate) containing 1.2% of agar in HSA medium. The gold particles coated by plasmid DNA from pβE204Q and pWT-373 (Newman et al., 1990) were bombarded onto the CC-373 cells using the Biolistics PDS-1000 Particle Delivery System (Du Pont-New England Nuclear). The bombarded cells were stored in the dark overnight and then transferred to the 1.2% agar plates with 100 μg of spectinomycin per mL of HSA medium.

Single colonies that appeared on the spectinomycin-containing CC plates were streaked on new plates with the same media. Southern blot analysis as per Sambrook et al. (1989) was used to verify the presence of homoplasmic cell lines. DNA from transformed cells was isolated by using a rapid DNA mini-preparation procedure as per Newman et al. (1990). A ^{32}P-labeled 8.0 kb *Bam*-10.3 chloroplast DNA fragment was prepared as the probe of the Southern blot by using a Multiprime DNA Labeling kit (Amersham). This transfer of single colonies to new spectinomycin-containing CC plates and Southern blot analysis as per Webber et al. (1993) was repeated until homoplasmic cell lines were obtained. Final confirmation that the cell line contained the mutant was made by cycle sequencing (Bethesda Research Laboratories).

Photoautotrophic Competence. The growth curves of all three different *C. reinhardtii* strains were measured by the change in optical density (cell scattering) at 720 nm under photoautotrophic conditions. Each liter of culture medium contained 5 mL of Beijerinck's stock solution, 5 mL of phosphate stock solution, and 1 mL Hunter trace elements solution (Harris, 1989). Cells were grown at 25 °C at a light intensity of 80 μE M^{-2} s^{-1}.

Preparation of Coupled Thylakoid Membranes. The methods used for preparation of thylakoid membranes have been described previously (Selman-Reimer et al., 1981). Cultured cells in 500 mL volume ($OD_{650nm} \approx 1$) were collected after spinning at 200*g* for 5 min. The pellet was washed with 100 mL of 50 mM Tricine-NaOH (pH 7.8−8.0) at 4 °C. When used for ATPase assay, the cells were disrupted by using a French press at the pressure of 1000 psi, and the suspension was centrifuged to remove the unbroken cells. When used to assay for rates of photophosphorylation or ATPase-driven proton pumping, the cells were resuspended in 50 mM Tricine-NaOH (pH 8.3), 40 mM NaCl, 5 mM $MgCl_2$, and 0.25 M sucrose at a concentration of 0.5 mg of chlorophyll per mL and were broken by passing through the Bio-Neb cell disruption system (Glas-Col Wins R&D 100) at a flow rate of 10 mL/min at 90 psi. The disrupted cells were spun at 480*g* for 10 s, and 1.5 mL of supernatant was transferred to each centrifuge tube. Thylakoid particles were pelleted at 30 000*g* for 10 min. The thylakoids prepared for the photophosphorylation assay were maintained at 4 °C in the dark after disruption of cells.

Isolation of C. reinhardtii CF_1-ATPase. The isolation of *C. reinhardtii* CF_1-ATPase followed the methods as reported in (Selman-Reimer et al., 1981). The thylakoid particles were washed with 10 mM sodium pyrophosphate four times at 4 °C. The thylakoid membranes were resuspended in 0.75 mM EDTA (pH 7.2−7.5) and stirred for 15 min at room temperature. The suspension was centrifuged at 30 000*g* for 40 min. The supernatant was collected and extracted with EDTA three times. The supernatant was then added to DEAE Sephadex A-50 equilibrated in 20 mM Tris-NaOH (pH 8.0), 10 mM ammonium sulfate, and 1 mM EDTA. The suspension was stirred slowly for 30 min at room temperature. The protein was eluted from the resulting DEAE Sephadex column with 300 mL of 20 mM Tris-NaOH (pH 8.0), 1.0 mM ATP, 2 mM EDTA, and 300 mM ammonium sulfate. The fractions containing the highest concentration

of protein were stored as a precipitate in a 50% saturated solution of ammonium sulfate at 4 °C.

Protein concentration was determined by the Bradford reagent using bovine serum albumin as the standard. Subunit analysis of the purified CF_1 was made by SDS−PAGE using a 12% gel, and silver-staining as per Sambrook et al. (1989).

ATPase and ATPase-Driven H^+-Pumping Assays. The ATPase activity was determined using the coupled ATPase assay described in Harris (1987). The reaction mixture contained 1 μg of enzyme in 20 mM Tricine-NaOH (pH 8.0), 10 mM KCl, 1 mM EDTA, 2 mM phosphoenolpyruvate, 0.1 mM NADH, 30 units of lactic dehydrogenase, and 30 units of pyruvate kinase in 0.2 mL total volume. The isolated *C. reinhardtii* CF_1 was desalted over a spin column using 100 mM Tris-NaOH (pH 7.5) to resuspend the ammonium sulfate precipitated protein. To activate the CF_1, 50 mM dithiothreitol and 1% ethanol by total well volume were added directly to the reaction mixture. Assays were run for 5 min at 37 °C at 340 nm by using the negative kinetics program (Softmax) in the microtiter plate reader. Rate of reaction was determined by calculating the slope of initial rate of the reaction, typically in the first 20−30 s after adding the protein into the reaction mixture.

ATPase-driven H^+-pumping was measured by the quenching of 9-aminoacridine fluorescence as per Casadio et al. (1995). The reaction mixture contained 40 μg of coupled thylakoids in 50 mM Tricine (pH 8.5), 50 mM KCl, 5 μM 9-aminoacridine, 10 mM dithiothreitol, and the concentrations of $MgCl_2$ and ATP indicated in 2 mL total volume. Fluorescence of 9-aminoacridine was measured at 25 °C using a Spex spectrofluorimeter (DM3000) with excitation and emission wavelengths set at 400 and 450 nm, respectively.

Photophosphorylation/F_1F_0-Reconstitution Assays. Photophosphorylation was measured as described in Selman-Reimer et al. (1981). The isolated thylakoid membranes were resuspended in 1 mL of 50 mM Tricine-NaOH (pH 8.3), 40 mM NaCl, and 5 mM $MgCl_2$. The concentration of the chlorophyll was measured spectrophotometrically in 80% acetone (Inskeep & Bloom, 1985). Rates of PMS-dependent photophosphorylation were determined with 10 μg of dark-adapted *C. reinhardtii* thylakoids in 100 μL of reaction mixture containing 50 mM Tricine-NaOH (pH 8.3), 10 mM NaCl, 0.5 mM $MgCl_2$, 2 mM NaH_2PO_4, 2.6×10^5 cpm of $^{32}P_i$, 2 mM ADP, 25 mM dithiothreitol, and 0.08 mM phenazine methylsulfate (PMS). The reaction mixtures were illuminated by an Oriel-66181 lamp at 25 °C. The reaction was stopped by adding 900 μL of a 4:1 (v:v) mixture of 70% $HClO_4$ and 5% ammonium molybdate. The synthesized [γ-^{32}P]ATP was extracted and separated from free [^{32}P]phosphate three times by using a 1:1 (v:v) mixture of benzene and water-saturated isobutanol. The organic phase was removed, and 100 μL of the aqueous phase was collected. The amount of the synthesized [γ^{32}P]ATP was measured with a Wallac 1410 liquid scintillation counter.

All steps for the depletion and reconstitution of CF_1 from thylakoids were carried out at 4 °C in darkness. Thylakoids were partially depleted of CF_1 according to Hesse et al. (1976) by washing thylakoids in buffer containing 10 mM Tris-Tricine (pH 8.0) and 10 μM $CaCl_2$ after three washes in 10 mM sodium pyrophosphate (pH 8.0). The CF_1-depleted thylakoid pellets were resuspended 50 mM Tricine (pH 8.3), 40 mM NaCl, and 5 mM $MgCl_2$. Reconstitution of CF_1 with partially depleted membranes was carried out as per Selman et al. (1978) in a 0.25 mL volume that contained 20 μg of thylakoids, 50 mM Tricine (pH 8.3), 2 mM NaCl, 20 mM $MgCl_2$, 0.25 M sucrose, and 30 μg of isolated CF_1. The suspensions were stirred in darkness for 1 min at 19 °C, then diluted to 1.5 mL with the same buffer, and assayed for photophosphorylation.

Electron Transfer Assays. The PSI-dependent electron transfer activity was measured polarographically using YSI 5331 oxygen probe at 25 °C. Light-dependent oxygen consumption was measured in the presence of 50 μM methyl viologen, 100 μM 2,6-dichlorophenolindolphenol, 10 μM 3-(3,4-dichlorophenyl)-1,1-dimethylurea, 5 mM ascorbic acid, and 50 mM Tricine-NaOH (pH 8.0). Samples were illuminated using an Oriel 6358 lamp with a 600 nm cutoff filter.

EPR Measurements and Sample Preparation. EPR samples were prepared as described earlier (Houseman et al., 1994a) except that the protein was not first precipitated. Rather, the volume of isolated *C. reinhardtii* CF_1-ATPase eluted from the DEAE Sephadex A-50 column was concentrated to 5 mL on an Amicon XM-100 membrane. The metal and the nucleotide from site 3 of this protein were then depleted by adding the CF_1 to a Sephadex G-50 column equilibrated in 50 mM HEPES (pH 8.0), 1 mM ATP, and 500 mM NaCl. Consequently, the N2 noncatalytic site of this CF_1 was not depleted. The elutent was reconcentrated and rediluted several times to reach a volume of 0.3 mL in 50 mM HEPES (pH 8.0), 1 mM ATP, and 175 mM NaCl buffer. This salt concentration was found to be the minimum that allowed the *C. reinhardtii* CF_1 to be concentrated to 100−200 mg/mL without coagulation. In this respect the protein was different from spinach CF_1 which did not require salt for stability in solution.

CW-EPR experiments were carried out at X-band (9 GHz) using a Bruker 300E spectrometer and a liquid nitrogen flow cryostat operating at 100 K. Simulations of the CW-EPR spectra employed the program QPOWA (Nilges, 1979; Maurice, 1980) which was the generous gift of J. Telser (Houseman et al., 1994a).

Preparation of VO^{2+} Solutions. Vanadyl was added in stoichiometric amounts to latent, metal−nucleotide-depleted CF_1 using a solution of freshly prepared $VOSO_4$ from which dissolved molecular oxygen had been removed by purging with dry nitrogen gas. VO^{2+} was added to a solution of ATP at pH 8.0 in a 1.0:1.0 mole ratio.

RESULTS

Mutagenesis and Chloroplast Transformation. The *atpB* gene, encoding the CF_1 β-subunit of *C. reinhardtii*, is located in the chloroplast DNA restriction enzyme fragment *Bam*-10. The *Eco*RI−*Bam*HI fragment isolated from *Bam*-10, which we designated *Bam*-10.3, was subcloned into pUC19. A 2.9 kilobase pair (kb) *Eco*RI−*Kpn*I fragment from *Bam*-10.3 was used for mutagenesis as described in methods. The *atpA-aadA-rbcL* gene that confers spectinomycin resistance was then subcloned into the *Kpn*I site and replaced the 1.15 kb *Kpn*I fragment to create *Bam*-10-*aadA-rbcL* (Bingham & Webber, 1994). A restriction enzyme map of *Eco*RI−*Bam*HI of chloroplast DNA restriction enzyme fragment *Bam*-10 and the locations of inserted *atpA-aadA* cassette and mutated residues are shown in Figure 1. The CC-373

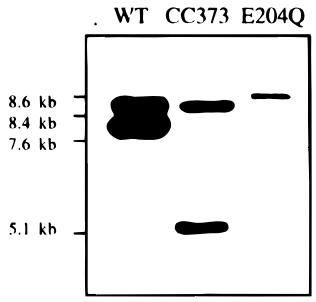

FIGURE 2: Autoradiogram of a Southern blot of total cellular DNA from wild-type and mutant cells. Isolated DNA was digested with *Bam*HI, separated on a 0.8% agarose gel, and probed with *Bam*-10.3 chloroplast DNA fragment. The DNA used in each lane is from cells of WT, wild-type CC-125; CC373, recipient CC-373; E204Q, the βE204Q mutant.

strain of *C. reinhardtii* contains the chloroplast au-u-c-221 mutation, a 2.5 kb deletion of *Bam*-10 including the 3′ end of the *atpB* gene. Complementation of the CC-373 strain with *Bam*-10-*aad*A provided the means to make site-directed mutations into the *atpB* gene using spectinomycin resistance as a selectable marker.

Figure 2 shows a Southern blot of DNA to determine whether the colonies from the mutant were homoplasmic for the inserted *Eco*RI−*Kpn*I fragment after several rounds of single colony selection. This blot, containing the *Bam*HI digest of the miniprep-purified DNA, was probed with the labeled DNA plasmid *Bam*-10.3. With a wild-type DNA (lane 1), the probe hybridized to a 7.6 kb band corresponding to *Bam*-10 and an 8.4 kb band corresponding to *Bam*-9. The latter fragment was visible because part of *Bam*-9 is homologous to *Bam*-10 sequences in the other copy of the inverted repeat (Bingham & Webber, 1994). With DNA isolated from CC-373 (Lane 2), the probe hybridized to an 8.4 kb band corresponding to *Bam*-9 and a 5.1 kb band corresponding to *Bam*-10. Due to the 2.15 kb spectinomycin resistance gene used to replace the 1.15 kb *Kpn*I fragment, the mutant (lane 3) showed an 8.6 kb band. However, the 9.4 kb *Bam*-9 fragment with the inserted *atpA-aadA-rbcL* cassette was not observed in the mutant due to reduced homology between *Bam*-9 and the probe after removing the 1.15 kb *Kpn*I fragment. Only the 8.6 kb band could be observed in the mutant, indicating that all copies of *Bam*-10 integrated the mutated gene.

To verify further the existence of the appropriate mutation in the transformants, the region containing the mutation was amplified from total cellular DNA by polymerase chain reaction (PCR). The PCR product was directly sequenced to confirm the presence of the desired mutation which was found to contain the desired base change (data not shown).

Photoautotrophic Growth Rates. Growth curves of wild type and mutant strains under photoautotrophic conditions were measured as shown in Figure 3. Wild-type and WT-373, the CC-373 strain complemented to a photosynthetic strain by transformation with wild-type *Bam*-10, showed comparable growth rates with doubling times of 19 and 20 h, respectively. These growth rates were somewhat slower than previously reported (Harris, 1989) since cells were grown under low light to prevent possible photoinhibitory effects of higher light intensities in the mutants. The 2.5 kb *atpB* deletion strain CC-373 was unable to grow under photoautotrophic conditions, as were cells that contained the mutation at βE204. The difference in photoautotrophic

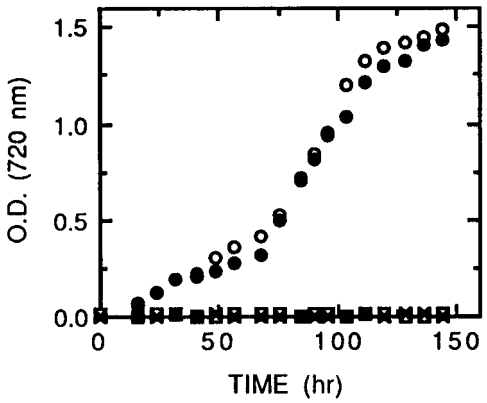

FIGURE 3: Photoautotrophic growth curves of wild-type and mutant *C. reinhardtii* strains. Cells were grown at 25 °C at a light intensity of 80 μE M^{-2} s^{-1} and measured as the optical density (cell scattering) of the liquid culture at 720 nm: wild-type (○), WT-373 (●), βE204Q (□), and CC-373 (×).

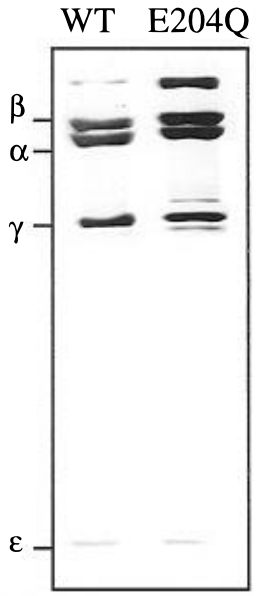

FIGURE 4: Analysis by SDS−PAGE of the polypeptide constituents of CF_1 preparations purified from wild-type and mutant *Chlamydomonas*. A 12% acrylamide, silver-stained gel was used to visualize polypeptides from wild-type (WT) and mutant cells as indicated.

growth between wild-type and mutants suggests that these changes in the β subunits of CF_1 have a significant effect on ATP synthesis.

Yield and Composition of Mutant CF_1. To determine whether the mutation affected the assembly of CF_1, the CF_1-ATPase was isolated from both wild-type and mutant, and was analyzed by SDS−polyacrylamide gel electrophoresis. No significant differences in the yield of purified protein were observed in the cells containing the site-directed mutant from the wild-type. Analysis of the subunit composition of purified CF_1 by SDS-PAGE is shown in Figure 4. No substantial difference between wild-type and mutant CF_1 was observed such that the mutant (lane 2) contained the α, β, γ, and ϵ subunits as did the wild-type (lane 1). The abundance of the δ subunit relative to the other subunits was variable among preparations. This subunit is known to be weakly associated with the *Chlamydomonas* CF_1 and is easily lost when the enzyme preparation is stored (Merchant et al., 1983). The variability of the abundance of the δ subunit did not appear to differ from that of wild-type CF_1. Other

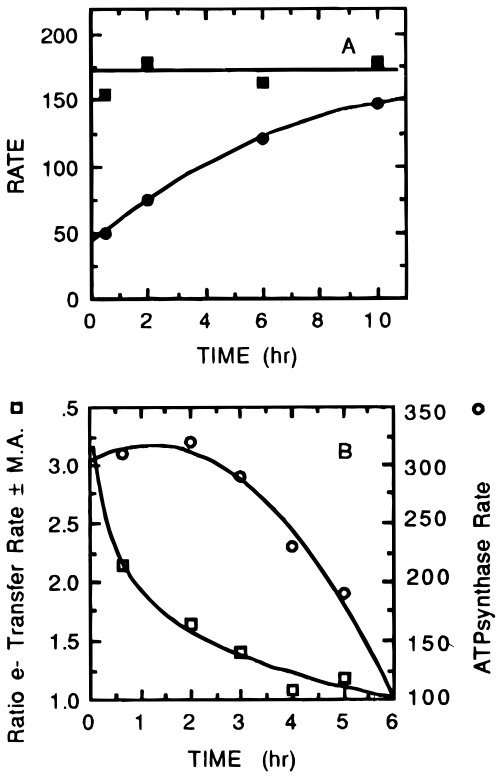

FIGURE 5: (A) Effect of the uncoupler methylamine on the rate of photosystem I-dependent electron transfer as a function of the age of thylakoids purified from wild-type *C. reinhardtii*. Thylakoid preparation and the methyl viologen-dependent electron transfer assay conditions were as described in Materials and Methods. The age of the thylakoids was measured from the time of cell disruption. The rate of electron transfer determined in the absence (●) or presence (■) of 30 mM methylamine is expressed as μmol of O_2 consumed (mg of Chl h)$^{-1}$. (B) Dependence of the rate of photophosphorylation on the ratio of uncoupled/coupled PSI-electron transfer as a function of the age of thylakoids purified from wild type *C. reinhardtii*. Rates were measured with isolated wild-type thylakoids as a function of time after cell disruption. Assay conditions for PSI-dependent electron transfer and PMS-dependent photophosphorylation are as described in Materials and Methods. The ratio of uncoupled/coupled PSI-electron transfer was determined as the fractional increase in the rate of O_2 consumption upon addition of 30 mM methylamine. Rates of ATP synthesis are expressed as μmol of ATP (mg of Chl h)$^{-1}$. The rate of O_2 consumption in the absence of methylamine 1 h after cell disruption was 122 μmol of O_2 (mg of Chl h)$^{-1}$.

bands visible in these preparations are polypeptides that have been reported previously to copurify with CF_1 from *Chlamydomonas* (Selman-Reimer et al., 1981).

Effect of the βE204Q Mutation on Energy Coupling. Following cell disruption, the stability of the thylakoids purified from *Chlamydomonas* in maintaining a proton gradient is limited. The ability to generate a proton gradient as a function of the age of the purified thylakoids was monitored by the increase in the rate of photosystem I (PSI)-dependent electron transfer upon addition of the uncoupler methylamine. As shown in Figure 5A, the rate of uncoupled electron transfer through PSI remained stable for more than 10 h. In the absence of the uncoupler, the PSI-dependent rate was about 30% of the uncoupled rate shortly after purification of the thylakoids but increased to more than 80% of the uncoupled rate after 10 h. The thylakoids were completely uncoupled after 24 h (data not shown).

Figure 5B shows the correlation between the rate of photophosphorylation of thylakoids purified from wild-type

Table 1: Functional Comparison of Wild-Type and βE204Q Mutant Thylakoids

	doubling time (h)	ratio[a] (+MA/−MA)	rate[b] (ATPsyn)
WT	19	1.90 ± 0.30	257 ± 25
βE204Q	no growth	2.55 ± 0.25	1.5 ± 1.5

[a] The ratio of rates of electron transfer with/without the uncoupler methylamine is monitored by light induced oxygen consumption as described in Materials and Methods, and the average is from two determinations. [b] The unit of ATP synthetic rate is μmol of ATP (mg of Chlorophyll h)$^{-1}$, and the average is from three determinations.

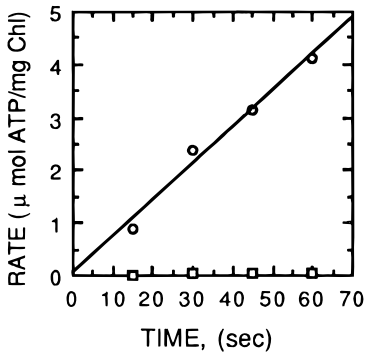

FIGURE 6: Comparison of PMS-dependent photophosphorylation activity of thylakoids purified from wild-type (○) and βE204Q (□) *C. reinhardtii*. mutant. Activities were measured within 30 min after cell disruption.

Chlamydomonas, and the ratio of uncoupled to coupled PSI-driven electron transfer as a function of the age of the purified thylakoids. The uncoupled rate of PSI-dependent electron transfer in this experiment was about 200 μmol of O_2 (mg of Chl h)$^{-1}$. The rate of photophosphorylation catalyzed by the purified thylakoids remained stable for about 3 h from the time that the cells were disrupted. The loss of coupling with time had a significant effect on the rate of photophosphorylation only after the ratio of uncoupled to coupled electron transfer decreased below 1.3.

In order to compare the effects of the mutation on the rate of photophosphorylation as shown in Table 1, the rates were determined within 30 min after cell disruption where the extent of uncoupling induced by thylakoid purification was not limiting to the photophosphorylation rate. Table 1 also shows the ratio of uncoupled to coupled PSI-driven electron transfer observed for purified thylakoids from the wild-type and the βE204Q mutant. The data show that thylakoids could be purified from the mutant with ratios that clearly exceeded the value of 1.3 necessary to obtain maximal rates of photophosphorylation. Thus, the mutation did not decrease the extent of coupling in the purified thylakoids relative to the wild-type.

Figure 6 shows the rate of photophosphorylation of the wild type and mutant with the purified thylakoids used to obtain the ratios of uncoupled to coupled PSI-driven electron transfer in Table 1. The rates remained linear in all cases for up to 5 min due to an ATP regenerating system. The calculated rates of ATP synthesis are also summarized in Table 1. Despite the fact that the membranes containing the βE204Q mutant were more tightly coupled than the thylakoids from the wild-type cells, they were unable to synthesize ATP. These results correlate closely with the inability of the mutant to grow photoautotrophically.

Table 2: Reconstitution of Photophosphorylation by the Addition of Purified F_1 to Wild-Type or βE204Q Mutant F_1-Depleted Thylakoids

	% rate of photophosphorylation			
treatment	wtF_1F_0	βE204-QF_1F_0	$wtF_1\beta$-E204QF_0	βE204-QF_1wtF_0
thylakoids before F_1-depletion	100	1		
F_1-depleted thylakoids	0	0		
reconstituted thylakoids	67	1	32	12

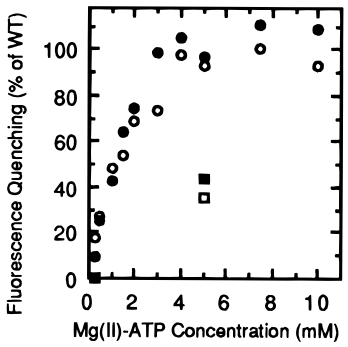

FIGURE 7: Mg^{2+}-ATP concentration dependence of the pH gradient generated in thylakoids by Mg^{2+}-ATPase activity by wild type (○) and βE204Q mutant (●) CF_1F_0. The data are expressed as the fractional extent of fluorescence quenching of 9-aminoacridine as described in Materials and Methods, using the maximal extent of quenching observed by the wild-type thylakoids as 100%. The extent of Mg^{2+}-ATPase-induced 9-aminoacridine fluorescence quenching by wild-type (□) and βE204Q mutant (■) CF_1F_0 in the presence of 5 mM NaN_3 is shown.

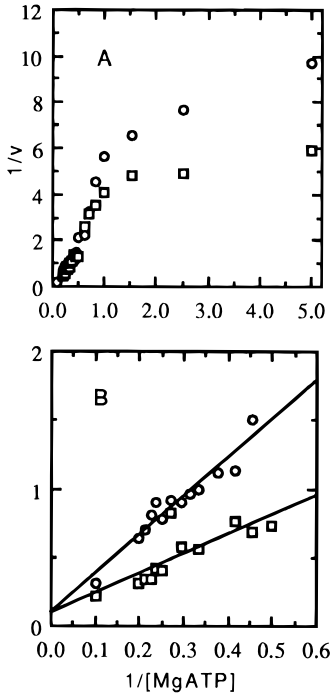

FIGURE 8: (A) Double-reciprocal plots for Mg^{2+}-ATPase activity of CF_1 purified from wild-type (○) and βE204Q (□) mutant of *C. reinhardtii*. The ratio of Mg^{2+}:ATP was maintained at 1:1 in all assays. Assay conditions were as described in Materials and Methods and activity is expressed as μmol of ATP (mg of CF_1 min)$^{-1}$. (B) Expansion of the data of A at higher substrate concentrations.

The inability of the mutant to synthesize ATP could result if the mutation caused F_0 to assemble incorrectly. The functional competency of the F_1 and F_0 componants was compared by the relative ability of purified F_1 to reconstitute ATP synthesis activity to F_1-depleted thylakoids. Removal of all of the CF_1 from thylakoids has been found to limit the extent of reconstitution of photophosphorylation upon addition of purified F_1 significantly (Hesse et al., 1976). To this end, 10 μM $CaCl_2$ was present during the F_1-depletion step to allow the membranes to retain a small fraction of the CF_1.

As shown in Table 2, addition of purified wild-type F_1 to F_1-depleted, wild-type thylakoids was able to reconstitute about 67% of the original ability of the membranes to catalyze photophosphorylation. Addition of wild-type F_1 to the F_1-depleted thylakoids from the mutant reconstituted about half of that observed in the control. The converse experiment, in which the mutant F_1 was reconstituted with the wild-type F_0, resulted in thylakoids that had 12% of the rate of photophosphorylation of the control. Since the mutant membranes were incapable of photophosphorylation either before depletion or after reconstitution, the small amount of activity observed in the βE204QF_1wtF_0-reconstituted membranes results from the residual wtF_1 that was not removed during the depletion step. These data indicate that the F_0 from the mutant is capable of coupling the proton gradient to catalyze the synthesis of ATP.

The ability of the mutant CF_1F_0 to catalyze ATPase-driven proton pumping in purified thylakoids is shown in Figure 7. The extent of fluorescence quenching of 9-amino acridine was used to estimate the pH gradient generated as a function of the concentration of Mg^{2+}-ATP. The data are expressed as a percent of the maximal extent of fluorescence quenching observed by the wild-type CF_1F_0. The mutation did not effect either the maximal extent of the gradient generated upon addition of Mg^{2+}-ATP or the Mg^{2+}-ATP concentration dependence on the size of the gradient. The ATPase-driven proton pumping by wild-type and mutant enzymes was also inhibited by azide to about the same extent, indicating that the fluorescence quenching was dependent on CF_1F_0. These results indicate that the mutant has not altered the machinery to catalyze ATPase activity and use it to pump protons across the thylakoid membrane.

Effects of the Mutations on ATPase Activity. Figure 8A shows a double-reciprocal plot for Mg^{2+}-ATPase activity of wild type and mutants. Under the conditions of the assay, the enzyme shows negative cooperativity similar to MF_1 kinetics. Figure 8B shows an expansion of the data at higher substrate concentrations where the double reciprocal plots approach linearity. Although the βE204Q mutation virtually eliminates photoautotrophic growth and photophosphorylation, the apparent k_{cat} of the ATPase reaction under steady state conditions was unaltered. The apparent k_{cat} and apparent k_{cat}/K_M of wild-type and mutant obtained from Figure 8B are summarized in Table 3. The βE204Q mutation increased the apparent k_{cat}/K_M by about 2-fold over the wild-type indicating an increase in the efficiency of the reaction under first-order conditions.

Figure 9A shows the dependence of ATPase activity of CF_1 purified from the wild-type and mutant on the Mg^{2+} concentration in the presence of 5 mM ATP. The concentration of Mg^{2+} which gave the highest rate of ATPase activity in both strains was 5 mM. At lower concentrations, the increase in the rate of ATPase as a function of Mg^{2+} was not significantly different between the mutant and wild-type

Table 3: Comparison of the ATPase Activity of Wild-Type and Mutants

	apparent k_{cat}[a]	apparent k_{cat}/K_M[b]
WT	69.0	2400
βE204Q	67.4	4700

[a] These data are calculated from Figure 9B, and the units of k_{cat} are s^{-1}. The estimated uncertainty is $\pm 3.3\ s^{-1}$. [b] These data are calculated from Figure 9B, and the units of k_{cat}/K_M are $M^{-1}\ s^{-1}$. The estimated uncertainty is $\pm 10\ M^{-1}\ s^{-1}$.

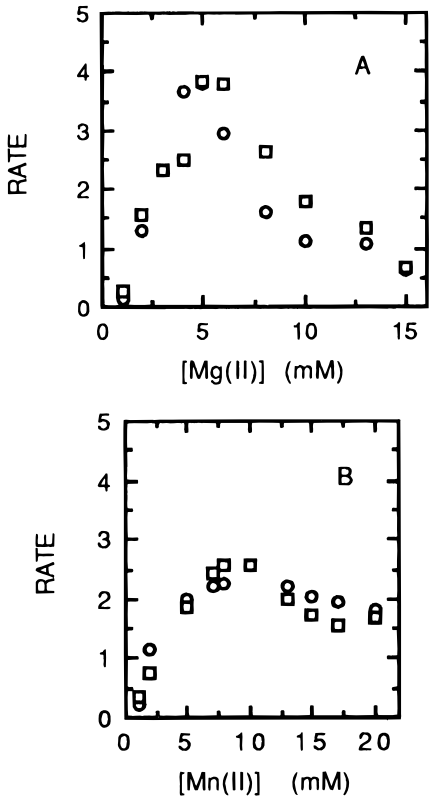

FIGURE 9: Comparison of the (A) Mg^{2+}-dependence and (B) Mn^{2+}-dependence of ATPase activity of CF_1 purified from wild-type (○) and βE204Q (□) mutant of *C. reinhardtii*. Assay conditions were as described in Materials and Methods using 5 mM ATP and the concentrations of Mg^{2+} or Mn^{2+} indicated. Rates of ATPase activity are expressed as μmol of ATP (mg of CF_1 min)$^{-1}$.

enzymes. As the concentration of Mg^{2+} was increased above 5 mM, the rate of ATPase activity decreased due to inhibition by metal not complexed with nucleotide. The CF_1 from both strains was inhibited roughly equally by free Mg^{2+}.

When Mn^{2+} was used as a cofactor for ATPase activity (Figure 9B), the wild-type and βE204Q mutant displayed the highest rates of ATPase activity at 10 mM Mn^{2+}. Somewhat lower rates of ATP hydrolysis were observed with Mn^{2+} than when Mg^{2+} was a cofactor. In addition, the presence of free Mn^{2+} did not result in the sharp decrease in ATPase activity caused by free Mg^{2+}. Thus, Mn^{2+} is not as effective a cofactor or inhibitor of the *Chlamydomonas* CF_1-ATPase as Mg^{2+}. However, the ability of Mn^{2+} either to activate or to inhibit the ATPase activity was the same in the mutant as in the wild-type. Thus, the dependence of ATPase activity on Mg^{2+} and Mn^{2+} suggests that βE204 is not directly responsible in binding the metal cofactor or in the nonproductive binding of the free metal that leads to inhibition.

Effects of the Mutation on the ^{51}V EPR Spectrum. The ^{51}V hyperfine coupling of VO^{2+} is a sensitive probe of the

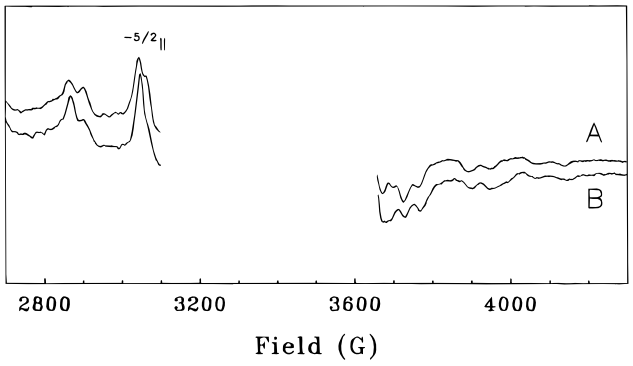

FIGURE 10: EPR spectrum of VO^{2+}-ATP at site 3 of (A) wild-type and (B) βE204Q mutant CF_1-ATPase. Conditions: microwave frequency, 9.553 GHz; field modulation, 7.86 G; scan rate, 10.4 G/s; time constant, 0.33 s; digital resolution, 2048 points; average protein concentration, 180 mg/mL; 1.0 VO^{2+}-ATP per CF_1. Trace A is an average of spectra from three different wild-type samples, each spectrum normalized before summation for signal intensity in order to weight each sample equally and thereby to account for differences in number of scans and protein/VO^{2+} concentration; average scans per sample, 240. Trace B is an average of spectra from four different βE204Q samples similarly normalized before summation; average number of scans per sample, 140.

types of groups that compose the equatorial ligands of a metal-binding site (Chasteen, 1981). Earlier analysis of VO^{2+} bound to catalytic site 3 of latent CF_1 in the "free-metal-inhibited" form, M3, indicated the presence of a single carboxylate ligand which is displaced upon activation (Houseman et al., 1994b, 1995). Two waters and a hydroxyl group from a serine or threonine compose the best fit for the remaining equatorial ligands to this species. If βE204 is the carboxyl group that serves as a ligand in the M3 form, then substituting a glutamine at this position could have three possible effects. First, if the glutamine does not coordinate, the amount of VO^{2+} that binds to the site could be significantly decreased. Second, lack of coordination by the glutamine side chain could lead to the ligation by water at this position. Such a change in ligation would change $A_{||}$ and $g_{||}$ by 8.8 MHz and 0.002, respectively. Third, a comparison of model complexes in which a carboxylate ligand to VO^{2+} is replaced by an amide has shown that there are small differences in the $A_{||}$ ^{51}V hyperfine coupling and in the $g_{||}$ value of about 3 MHz and 0.001, respectively (Colpas et al., in preparation). Thus, these same differences in hyperfine coupling and g value might be expected in the βE204Q mutant as compared to the wild type if this residue forms a ligand.

Figure 10 shows the EPR spectra of VO^{2+} bound to catalytic Site 3 of CF_1 purified from wild type (spectrum A) and the βE204Q mutant (spectrum B) of *Chlamydomonas*. These spectra are the normalized sums of spectra from three different samples of wild-type CF_1 and four different samples of βE204Q mutant CF_1. Two species of bound VO^{2+} are evident in this spectrum which can be discerned most clearly at the $-5/2_{||}$ resonances (Figure 11). Houseman et al. (1994b) determined that these species result from VO^{2+} bound at catalytic site 3 as free metal (M3) and as the metal−nucleotide complex (M3−N3).

As shown in Figure 10, no significant differences in resonance positions were observed between the spectra of the VO^{2+} bound to the CF_1 from the wild-type and the βE204Q mutant for either species of bound VO^{2+}. Neither were significant differences in the binding of VO^{2+} between

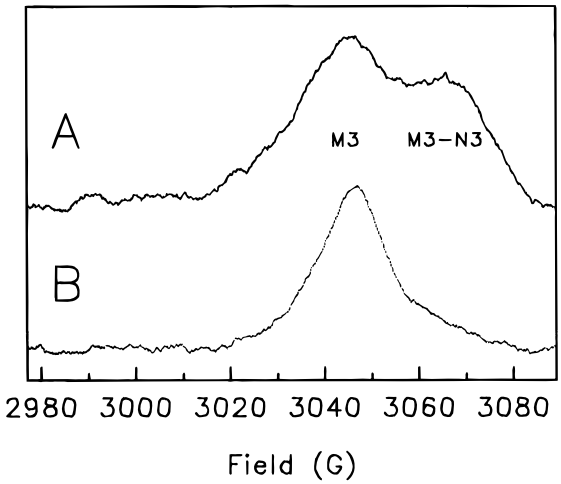

FIGURE 11: The $-5/2_{||}$ region of the EPR spectrum (as indicated in Figure 10) of (A) wild-type CF_1 and (B) βE204Q CF_1 showing both M3 and M3−N3 species of VO^{2+} coordinated to catalytic site 3. Each spectrum is the sum of spectra from three separate samples. Conditions: microwave frequency, 9.559 GHz; microwave power, 1.0 mW; field modulation, 4.96 G; scan rate, 5.37 G/s; time constant, 0.164 s; average protein concentration, 173 mg/mL for A and 156 mg/mL for B, 1.0 VO^{2+}-ATP per CF_1; average number of scans for each sample, 130. Base lines were subtracted from CF_1 spectra in both cases.

wild-type and mutant protein observed (data not shown). Simulation of the EPR spectrum of bound VO^{2+} in the M3 form using the program QPOWA determined that the parallel component of the ^{51}V hyperfine tensor, $A_{||}$, was 497 MHz, and that $g_{||}$ was 1.948 for both the wild-type and mutant, consistent with an equatorial carboxyl group.[2]

The absence of any significant changes in the hyperfine and g values of bound VO^{2+} as a result of the mutation clearly rules out the possibility that water has substituted for amide as a ligand to the metal. Although only a small difference in $A_{||}$ was expected between the wild type and the mutant, the lack of change also supports the results from the kinetics study in indicating that βE204 is not one of the equatorial ligands of the metal that gives rise to the free-metal-inhibited (or latent) form of the enzyme.

However, a difference in the relative intensities and therefore abundances of the M3 and M3−N3 species can be observed in the mutant and wild-type spectra of the latent enzyme (Figure 11). Although the ratio of intensities of M3 and M3−N3 in the latent form is variable in spinach (Houseman et al., 1994b) and *C. reinhardtii* CF_1, the M3−N3 species was even more intense in the *C. reinhardtii* wild-type than in spinach. In contrast, every sample of the mutant that was studied produced lower M3−N3 intensity than every wild-type sample. This difference between wild-type and mutant indicates that the βE204Q mutant binds a greater proportion of its metal−protein complex in the M3 "free-metal" form than does the wild-type.

DISCUSSION

The evidence presented here indicates that the loss of photoautotrophic growth observed in the βE204Q mutant is the result of the loss of the ability of the F_1-ATPase to phosphorylate ADP since the mutation did not affect: (i) the abundance of F_1 in the thylakoid membrane; (ii) the F_1 subunit composition; (iii) the functional assembly of F_1 with F_0; or (iv) the extent of coupling of the proton gradient with the electron transfer reactions. One of the proposed functions of βE204 was to serve as a ligand to the metals bound at the catalytic sites (Vallejos, 1981; Yoshida & Allison, 1986; Dagget et al., 1985; Park et al., 1994; Al-Shawi et al., 1990). However, this carboxyl group probably does not serve a role as a ligand to the metal under conditions in which the enzyme binds the metal−nucleotide complex productively or the free metal in a nonproductive manner due to the lack of significant changes in the βE204Q mutant in terms of (i) the ability of Mg^{2+} or Mn^{2+} to serve either as a cofactor or as an inhibitor of ATPase activity and (ii) the EPR spectroscopy of VO^{2+} bound to catalytic site 3.

We have used two approaches to understand the function of βE204. First, the effects of the βE204Q mutation on catalytic activity were examined. The results support a role for the βE204 carboxyl residue in serving to protonate the oxygen of the inorganic phosphate to make it a good leaving group and to facilitate nucleophilic attack by the β-phosphate oxygen of ADP during ATP synthesis. The ability of thylakoids purified from the βE204Q mutant to catalyze light-driven ATP synthesis was virtually nonexistent. The magnitude of the effect of the βE204Q mutation on ATP synthesis activity in this chloroplast enzyme was comparable to the mutation in the equivalent position of EF_1 (Park et al., 1994). Consistent with a role in catalysis, Abrahams et al. (1994) reported that the carboxyl group at the position equivalent to βE204 in the bovine mitochondrial F_1 is positioned in the catalytic site that contains bound AMP-PNP 4.4 Å from the γ-phosphate of the nucleotide with density for a bound water molecule that bridges these two groups.

This role for βE204 as a protonating catalytic group is supported not only by the absence of ATPsynthase activity in the βE204Q mutant, but also by the ineffectiveness of the mutation on the k_{cat} of the ATPase activity of purified CF_1. The enzyme is known to allow interconversion between ADP and ATP bound at the catalytic site without the net input of energy. Because this interconversion is rapid with respect to exchange of solvent and release of product, the bound ADP + P_i and ATP approach equilibrium with a K_{eq} that is close to unity (Boyer, 1993). The extent of the effect of removing the protonatable group from the site of catalysis is anticipated to be more profound on the ATPsynthase reaction than on the ATPase reaction since the former reaction requires the addition of protons that are in low abundance to the inorganic phosphate, but the latter reaction only requires hydrolysis by solvent water that is relatively abundant in the catalytic site. In the absence of the catalytic carboxyl group, the ATPase reaction should be able to proceed with even a somewhat limited access to the solvent. However, without the carboxyl group to position the protons needed for the ATPsynthase reaction, this reaction would be effectively blocked. Conversion of a rapidly reversible reaction to an irreversible one in the ATPase direction would result in a net increase in the k_{cat}/K_M of the steady-state ATPase reaction as observed.

Two studies have determined the rate constants of individual steps in the reaction under conditions in which

[2] This simulation of the M3 species is superior to that reported earlier (Houseman et al., 1994a,b) and yields exactly the same $A_{||}$ and $g_{||}$ values for spinach and for *C. reinhardtii* wild-type and βE204Q CF_1. These new values are still consistent with the coordination of a carboxylate ligand in the M3 species.

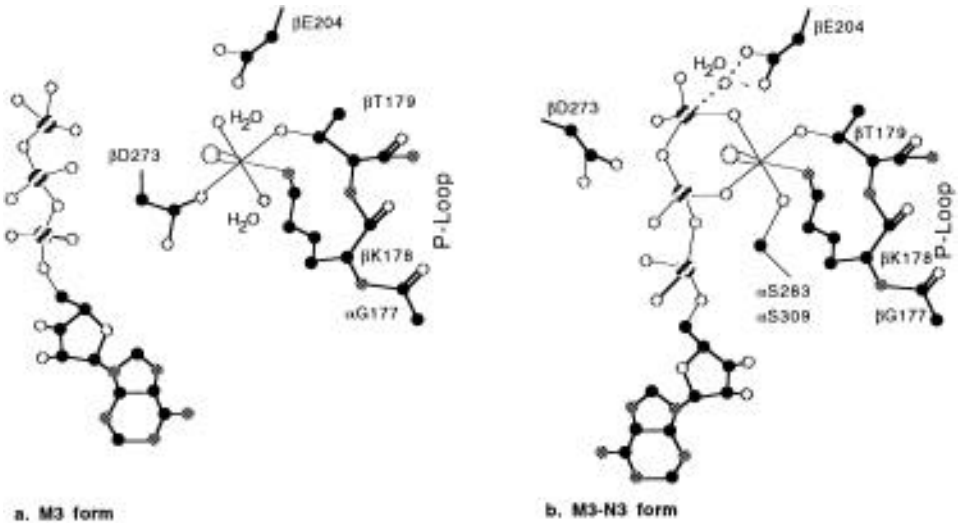

FIGURE 12: Representation of catalytic site 3 of latent CF_1 (a) in the M3 form where the bound nucleotide is not coordinated to the metal at this site and (b) in the M3−N3 (metal−nucleotide complex) form showing the best fit for the coordination environments based on Houseman et al. (1995) and the interaction of the nucleophilic water and βE204 in *C. reinhardtii* CF_1 (βE188 using the MF_1 sequence).

only one of the three catalytic sites is filled (Senior et al., 1992; Park et al., 1994).

$$F_1 + ATP \underset{k_{-1}}{\overset{k_{+1}}{\leftrightarrow}} F_1{<}ATP \underset{k_{-2}}{\overset{k_{+2}}{\rightleftharpoons}} F_1{<}ADP{\cdot}P_i \rightleftharpoons F_1{<}ADP + P_i \rightleftharpoons F_1 + ADP + P_i$$

These studies show that the rate constants of both the forward and reverse catalytic events are decreased by the mutation. However, even in the mutants, the rate-limiting step of the ATPase reaction under unisite conditions remains the release of products. The ratio of the rate constants for the interconversion of ATP with ADP (k_{+2}/k_{-2}) is shifted about 25-fold in favor of the formation of ADP and P_i (the ATPase direction) in the mutant from the wild-type (Senior et al., 1992; Park et al., 1994). Our multisite kinetic study on CF_1 agrees with the unisite studies on EF_1 in that neither the binding step nor the hydrolysis step is slowed by the mutation enough to become rate-limiting. Thus, this study of the βE204Q mutant F_1-ATPase in a eukaryotic system under multisite conditions is complementary to the studies of the same mutant in prokaryotic systems. Even so, the mutants equivalent to βE204Q that were made in prokaryotic systems have been examined for ATPase activity at 10 mM ATP which was decreased about 1000-fold from the concentration of the wild-type enzyme (Senior & Al-Shawi, 1992; Park et al., 1994). The only apparent reason for this large difference in the ability of the two enzymes with equivalent mutations it that the *Chlamydomonas* enzyme may have another protonatable group positioned near the catalytic site that can serve as a surrogate in hydrogen bonding to the inorganic phosphate which is not conserved in the *E. coli* enzyme. Such results exemplify the need to analyze mutations of the F_1-ATPase from disparate origins.

The second approach to understand the function of the βE204 residue in our study was to compare the EPR spectra of mutant and wild-type CF_1. Because of the sensitivity of the ^{51}V hyperfine coupling to changes in the VO^{2+} equatorial coordination environment, the absence of any significant effect on $A_{||}$ as a result of the βE204Q mutation implies that the coordination environment is essentially unchanged. Thus, either βE204 is not a ligand or else glutamine has almost exactly the same effect on $A_{||}$ as does glutamate. Although the couplings would be expected to be very similar, no significant difference could be detected at all, suggesting that βE204 is not a metal ligand.

The different ratios of the M3 to M3−N3 species from mutant and wild-type in the VO^{2+} EPR spectra are in agreement with this conclusion. Our earlier EPR evidence from spinach CF_1 (Houseman et al., 1994a,b) indicating that carboxylate binds only to the M3 form would imply that, if βE204 were this ligand, then mutating it to a glutamine should have its greatest effect in weakening the binding affinity of the site for metals and decreasing the EPR signal from the M3 form (Figure 12). Instead, this mutation favored M3 over the metal−nucleotide-bound form, M3−N3.

It would appear that the mutation had its greatest effect in lowering the affinity of the site for the M3−N3 form. The decrease in the relative abundance of the M3−N3 form in the βE204Q mutant lends further support to the idea that this residue interacts with the terminal phosphate or the nucleophilic water and not with the metal directly. The different ratios of M3 to M3−N3 in the wild-type and the mutant are probably the result of the different hydrogen bonding abilities of the glutamic acid and the glutamine side chains, and this difference may be enough to favor one form over the other in the latent state of the enzyme. If βE204 is not a metal ligand, but is both a catalytic proton donor and an important residue in the formation of the metal−nucleotide complex, then mutation of this glutamate to a glutamine would have essentially no effect on the free-metal-bound form, M3, but the mutation would be likely to destabilize the metal−nucleotide-bound form, M3−N3, as is observed.

Thus, this EPR investigation suggests that the βE204 residue in *C. reinhardtii* has the function of facilitating the coordination of the nucleotide phosphates to the metal in addition to that of protonating the phosphate. Our suggestion that the βE204 residue contributes to the stability of metal−nucleotide complex form in latent *C. reinhardtii* CF_1 agrees with the kinetic studies under unisite conditions of EF_1 discussed above (Park et al., 1994; Senior et al., 1992). Their analyses of the ATPase kinetics according to the above scheme implied that the βE204Q mutation hindered the ATP-

binding step by raising the free energy of the bound nucleotide relative to unbound nucleotide. (k_{+1} for the βE204Q mutant was less than that for the wild-type, and k_{-1} for the mutant was greater than that for the wild-type.) In fact, the largest effect on catalysis in EF_1 was on the nucleotide-binding step with a much smaller effect on the rate constant of hydrolysis. This binding step is comparable to the VO^{2+}-nucleotide binding observed for latent *C. reinhardtii* CF_1 in our EPR study in which the ATP-coordinated form (M3−N3) was rendered less favorable by the same mutation. It would appear that βE204 is an important residue at the catalytic site at various stages during turnover, not only assisting in the hydrolysis step (k_{+2} above) but also influencing the binding affinity of the site before hydrolysis.

Further efforts are under way to create mutants of βE204 that will produce more profound shifts in the ^{51}V hyperfine coupling if this residue does ligate metal in the free-metal-inhibited form. However, as βE204 does not appear to contribute to the coordination sphere of VO^{2+} at site 3, the most likely candidate for the carboxylate ligand in the M3 form is βD273 in *Chlamydomonas* CF_1.

ACKNOWLEDGMENT

The authors thank Scott Bingham and Hyeonmoo Lee for valuable discussion and Bruce Selman's group for helpful technical advice.

REFERENCES

Abrahams, J. P., Leslie, A. G. W., Lutter, R., & Walker, J. E. (1994) *Nature 370*, 621−628.

Amano, T., Tozawa, K., Yoshida, M., & Murakami, H. (1994) *FEBS Lett. 348*, 93−98.

Bingham, S. E., & Webber, A. N. (1994) *J. Appl. Phycol. 6*, 239−245.

Boyer, P. D. (1993) *Biochem. Biophys. Acta 1140*, 215−250.

Boynton, J. E., Gillham, N. W., Harris, E. H., Hosler, J. P., Johnson, A. M., Jones, A. R., Randolph-Anderson, B. L., Robertson, D., Klein, T. M., Shark, K. B., & Sanford, J. C. (1988) *Science 240*, 1534−1538.

Bruist, M. F., & Hammes, G. G. (1981) *Biochemistry 20*, 6298−6305.

Casadio, R., Bernardo, S. D., Fariselli, P., & Melandri, B. A. (1995) *Biochim. Biophys. Acta 1237*, 23−30.

Chasteen, N. D. (1981) in *Biological Magnetic Resonance* (Berliner, L., & Reuben, J., Eds.) pp 53−119, Plenum Press, New York.

Dagget, S. G., Gruys, K. J., & Schuster, S. M. (1985) *J. Biol. Chem. 260*, 6213−6218.

Esch, F., Bohlen, P., Otsuka, A., Yoshida, M., & Allison, W. (1981) *J. Biol. Chem. 256*, 9084−9089.

Frasch, W. D. (1994) in *Photosynthesis of the Cyanobacteria* (Bryant, D. A., Ed.) Chapter 11, pp 361−380, Kluwer Academic Publishers, Dordrecht, The Netherlands.

Frasch, W. D., & Selman, B. (1982) *Biochemistry 21*, 3636−3643.

Goldschmidt-Clermont, M. (1991) *Nucleic Acids Res. 19*, 4083−4089.

Grubmeyer, C., Cross, R., & Penefsky, H. (1982) *J. Biol. Chem. 257*, 12092−12100.

Harris, D. A. (1987) in *Spectrophotometry and Spectrofluorimetry*: *A Practical Approach* (Harris, D. A., & Bashford, C. L., Eds.) pp 50−90, IRL Press, Oxford, England.

Harris, E. H. (1989) in *The Chlamydomonas Sourcebook: A Comprehensive Guide to Biology and Laboratory Use* (Harris, E. H., Ed.) pp 12−50, Academic Press, San Diego, CA.

Hesse, H.; Ladwig, R. J., & Strotmann, H. (1976) *Z. Naturforsch. 31c*, 445−451.

Houseman, A. L. P., Morgan, L., LoBrutto, R., & Frasch, W. (1994a) *Biochemistry 33*, 4910−4917.

Houseman, A. L. P.; LoBrutto, R., & Frasch, W. (1994b) *Biochemistry 33*, 10000−10006.

Houseman, A. L. P.; LoBrutto, R., & Frasch, W. (1995) *Biochemistry 34*, 3277−3285.

Hyndman, D. J.; Milgrom, Y. M., Bramhall, E. A., & Cross, R. L. (1994) *J. Biol. Chem. 269*, 28871−28877.

Inskeep, W. P., & Bloom, P. R. (1985) *Plant Physiol. 77*, 483−485.

Maurice, A. M. (1980) Ph.D. Thesis, University of Illinois, Urbana, IL.

Merchant, S., Shaner, S. L., & Selman, B. R. (1983) *J. Biol. Chem. 258*, 1026−1031.

Newman, S. M., Boynton, J. E., Gillham, N. W., Randolph-Anderson, B. L., Johnson, A. M., & Harris, E. H. (1990) *Genetics 126*, 875−888.

Nilges, M. J. (1979) Ph.D. Thesis, University of Illinois, Urbana, IL.

Park, M. Y., Omote, H., Maeda, M., & Futai, M. (1994) *J. Biochem. 116*, 1139−1145.

Parsonage, D., Wilke-Mounts, S., & Senior, A. (1988) *FEBS Lett. 232*, 111−114.

Pougeois, R., Satre, M., & Vignais, P. (1979) *Biochemistry 18*, 1408−1413.

Sakurai, H., Iwashima, H., Hosoda, T., & Hisabori, T. (1989) *Seikagaku 61*, 1098.

Sambrook, J., Fritsch, E. F., & Maniatis, T. (1989) in *Molecular Cloning: A Laboratory Manual*. (Sambrook, J., Ed.) pp 9.31−9.55. Cold Spring Harbor Laboratory Press, Cold Spring Harbor, NY.

Selman, B. R., & Durbin, R. D. (1978) *Biochim. Biophys. Acta 502*, 29−37.

Selman-Reimer, S., Merchant, S., & Selman, B. R. (1981) *Biochemistry 20*, 5476−5482.

Senior, A. E., & Al-Shawi, M. K. (1992) *J. Biol. Chem. 267*, 21471−21478.

Senter, P., Eckstein, F., & Kagawa, Y. (1983) *Biochemistry 22*, 5514−5518.

Shoshan, V., & Selman, B. R. (1980) *J. Biol. Chem. 255*, 384−389.

Sueoka, N. (1960) *Proc. Natl. Acad. Sci. U.S.A. 46*, 83−91.

Vallejos, R. (1981) in *Energy Coupling in Photosynthesis* (Selman, B. R., & Selman-Reimer, S., Eds.) pp 129−139, Elsevier Holland, Amsterdam, The Netherlands.

Walker, J. E., Fearnley, I. M., Gay, N. J., Gibson, B. W., Northrop, F. D., Powell, S. J., Runswick, M. J., Saraste, M., & Tybulewicz, V. L. J. (1985) *J. Mol. Biol. 184*, 677−701.

Webb, M., Grubmeyer, C., Penefsky, H., & Trentham, D. (1980) *J. Biol. Chem. 255*, 11637−11639.

Webber, A. N., Gibbs, P. B., Ward, J. B., & Bingham, S. E. (1993) *J. Biol. Chem. 268*, 12990−12995.

Woessner, J. P., Gillham, N. W., & Boynton, J. E. (1986) *Gene 44*, 17−28.

Yoshida, M., & Allison, W. S. (1986) *J. Biol. Chem. 261*, 5714−5721.

Yoshida, M., Poser, J., Allison, W., & Esch, F. (1981) *J. Biol. Chem. 256*, 148−153.

BI961105A